Advanced laboratory testing of a sand-resin mixture liquefaction mitigation measure

Test avancé en laboratoire d'une mesure d'atténuation de la liquéfaction d'un mélange sable-résine

Luís Miranda, Laura Caldeira & João Bilé Serra
Departamento de Geotecnia, Laboratório Nacional de Engenharia Civil, Lisboa, Portugal, lmiranda@lnec.pt
Rui Carrilho Gomes
Departamento de Engenharia Civil, Instituto Superior Técnico, Universidade de Lisboa, Lisboa, Portugal

ABSTRACT: In the framework of a third Tagus River crossing, through an immersed tunnel, a novel liquefaction mitigation measure, namely injection of a duromeric expansive polyurethane resin, was tested on its highly liquefiable foundation sand. Three laboratory injection tests were executed: the first consisted in injecting a central column, inside a specifically designed box filled with Tagus River sand, to characterize the properties of the sand-resin mixture (SRM); the second and third comprised injecting five separate columns each, with different replacement ratios, to measure the effect of the injection on the sand densification between columns. An injection rod withdrawal rate (IRWR) of 0.01 m/90 s, 0.01 m/10 s and 0.01 m/15 s was used for the first, second and third tests, respectively. Specimens were core drilled from the injection test's columns, SRM behaving like a single-phase material. To characterize the SRM cyclic behaviour and to provide high quality data, essential to calibrate advanced constitutive models used in the design of the tunnel, laboratory tests were performed on the specimens, of which four cyclic torsional tests are presented in this paper, using two specimens from the columns of the second and third tests, respectively (base and top). In these tests, imposed strain increased progressively up to the maximum strain that could be applied in LNEC's torsional shear device, without slipping at the top of the specimen. Therefore, it was possible to analyse the amplitude, damping ratio and shear modulus of the cycles and characterize some elastic properties of the SRM.

RÉSUMÉ : Dans le cadre d'une troisième traversée du Tage, à travers par un tunnel immergé, une nouvelle mesure d'atténuation de la liquéfaction, à savoir l'injection d'une résine polyuréthane expansive duromérique, a été testée sur son sable de fondation hautement liquéfiable. Trois tests d'injection en laboratoire ont été réalisés: le premier a consisté à injecter une colonne centrale, à l'intérieur d'une boîte spécialement conçue remplie de sable du Tage, pour caractériser les propriétés du mélange sable-résine (SRM); les deuxième et troisième consistaient à injecter chacune de cinq colonnes séparées, avec des taux de remplacement différents, pour mesurer l'effet de l'injection sur la densification du sable entre les colonnes. Un taux de retrait de la tige d'injection (IRWR) de 0,01 m/90 s, 0,01 m/10 s et 0,01 m/15 s a été utilisé pour les premier, deuxième et troisième tests, respectivement. Les éprouvettes ont été carottées à partir des colonnes du test d'injection, le SRM se comportant comme un matériau monophasé. Pour caractériser le comportement cyclique du SRM et fournir des données de haute qualité, indispensables pour calibrer les modèles constitutifs avancés utilisés dans la conception du tunnel, des essais en laboratoire ont été réalisés sur les éprouvettes, dont quatre essais de torsion cyclique sont présentés dans cet article, à l'aide de deux éprouvettes à partir des colonnes des deuxième et troisième essais, respectivement (base et haut). Dans ces essais, la déformation imposée a augmenté progressivement jusqu'à la déformation maximale qui pouvait être appliquée dans le dispositif de cisaillement par torsion du LNEC, sans glisser dans le haut de l'éprouvette. Par conséquent, il a été possible d'analyser l'amplitude, le rapport d'amortissement et le module de cisaillement des cycles et de caractériser certaines propriétés élastiques du SRM.

KEYWORDS: cyclic torsional testing, liquefaction, mitigation measure, sand-resin mixture, Tagus River sand.

1 INTRODUCTION

Design of a third Tagus River crossing is currently being considered downstream of 25 de Abril Bridge in Lisbon, Portugal, in an area of high seismicity. The crossing would correspond to an immersed tunnel, between Algés and Trafaria, with a length of approximately 2.4 km.

Several immersed tunnels are built on alluvial formations in earthquake zones and one of the crucial issues in their design is their resistance to alluvial foundation liquefaction. Actually, the displacements of an immersed tunnel due to a seismic event depend essentially on the behaviour of the surrounding ground, namely its stiffness (Ingerslev and Kyiomya, 1997). These displacements may be amplified by liquefaction and lead to ground failure if substantial decrease of soil strength arises. Loss of lateral or vertical support, differential movements or rotations, movements due to shake-down settlement and floatation of the tunnel are significant consequences of liquefaction. The uncontrolled movement of the tunnel could also result in overstressing and damage of the structure or leakage of its joints. Therefore, liquefaction phenomena shall be avoided and efficient mitigation measures shall be implemented.

Concerning immersed tunnels, the viable options are to improve soil strength, density and/or drainage conditions in order to reduce ground susceptibility to liquefaction. The main recognized ground improvement techniques that have been applied to immersed tunnels include gravel drains, vibro-replacement, vibro-compaction and soil-cement columns (Lunniss and Baber, 2013).

Injection of expansive polyurethane resins is a recent mitigation measure, which was studied with the goal of enabling its future application, namely in immersed tunnel foundations. Expansive polyurethane resins are produced from an exothermic reaction, during which a great quantity of carbon dioxide is generated, determining the volumetric expansion of the mixture. In a very short period of time the mixture hardens, passing from a liquid to a solid state. After this, the mixture behaves like a single-phase material, in contrast with soil behaviour. Consequently, in the presence of a confinement, the expansive capacity of the resin produces densification of the surrounding soil, as additional material is introduced into a relatively constant soil volume. Besides, other effects, such as improvement in composite stiffness, cementation and horizontal stress increase, are also present. The combined effect provides a substantial improvement of ground strength in the injection zone, which is paramount in case of sand with high liquefaction

potential, like the Tagus River sand, and also to support the tunnel.

Soil consolidation treatment with expansive resins is not very invasive and has shown great flexibility, low energy consumption and extremely reduced environmental impacts. Although the cost of the resin may be considerable, even if controllable by restraining the volume of resin injection, the costs of operation of equipment are lower than most methods.

Moreover, Erdemgil *et al*. (2007), Manassero *et al*. (2016) and Traylen (2017) have proven that expansive polyurethane resin injection is a viable ground improvement method for liquefaction mitigation, as it led to elimination or a substantial reduction of liquefaction susceptibility.

A duromeric (closed cell) polyurethane resin, MC-Injekt 2700 L® (MC-Bauchemie, 2014), was studied for the first time in liquefaction mitigation (Miranda, 2019). Although being marginally less expansive, it has a much higher compressive strength and flexural tensile strength (around 5 times) and density (at least twice) than the Uretek® (Uretek Worldwide, 2014) elastomeric (open cell) resin.

In this paper, after the physical characterization of the Tagus River sand and of the MC-Injekt 2700 L® expansive polyurethane resin, the laboratory testing is described, including the testing plan and the specimen preparation techniques, which are thought specifically for this new application of the resin in liquefaction mitigation. Results from cyclic torsional tests are presented. The amplitude, damping ratio and shear modulus of the cycles are analyzed and some elastic properties of the SRM are characterized.

2 MATERIALS, SPECIMEN PREPARATION, TESTING PLAN AND EQUIPMENT

2.1 *Tagus River sand*

The immersed tunnel herein considered is supported on alluvial Tagus River sand, overlaying Miocenic layers of increasing stiffness and strength with depth and a basalt bedrock. The sand layer has a maximum thickness of around 50 m and the maximum river depth is about 30 m (Figure 1).

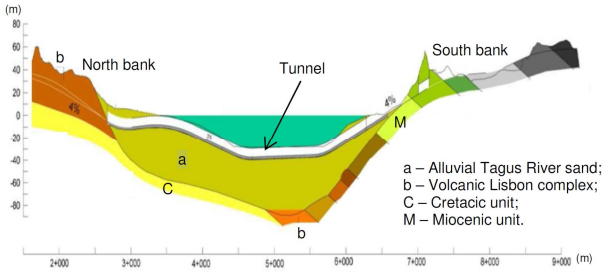

Figure 1. Third Tagus River crossing geologic profile.

Tagus River sand is a siliceous, clean and poorly graded sand, classified as SP according to the Unified Soil Classification System - ASTM D2487-17 (ASTM, 2017). After being dredged from the bottom of the river, it came with shells and small pebbles, which were removed by using the 2 mm sieve.

The sand physical characterization comprised: a grain size analysis; determining the solid particles density, G_S, and the maximum, $\gamma_{d,max}$, and minimum, $\gamma_{d,min}$, dry unit weight, according to ASTM D4253-16 (ASTM, 2016) and ASTM D4254-16 (ASTM, 2016) standards. The grain size distribution is shown in Figure 2, while other physical indexes are presented in Table 1.

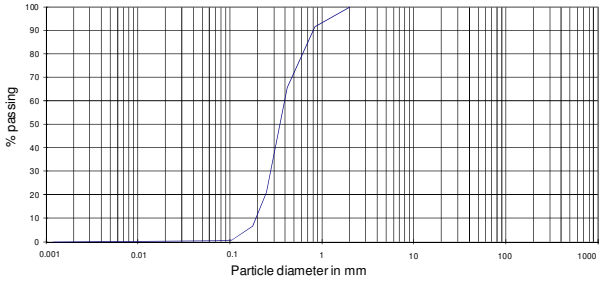

Figure 2. Grain size distribution for Tagus River sand after removal of large particles.

Table 1. Physical indexes of Tagus River sand

Physical index	*Value*	*Unit*	Physical index	*Value*	*Unit*
D_{10}	0.20	mm	C_u	2.00	-
D_{30}	0.28	mm	C_c	1.00	-
D_{50}	0.36	mm	G_S	2.70	-
D_{60}	0.40	mm	$\gamma_{d,max}$	17.12	kN/m^3
			$\gamma_{d,min}$	14.32	kN/m^3

The in-situ relative density, D_r, of Tagus River sand was determined by means of a correlation with SPT values (Skempton, 1986), obtained for different boreholes and depths, mainly in the north bank of the river, during geotechnical surveys between September 1999 and November 2007, kindly provided by Administração do Porto de Lisboa (Miranda, 2019). Similar SPT values were assumed at the centre of the river as, at the tunnel site, flow velocities near the bed of the waterway are small. The correlation is basically valid up to a depth of around 20 m below the riverbed, which corresponds to the main liquefiable soil zone in this case study. Based on this correlation, and with an average N_{SPT} of around 17, an estimated D_r of 70% was used in the laboratory tests. Furthermore, the characteristics and liquefaction conditions of the sand, for D_r between 60% and 80%, were studied through cyclic undrained torsional tests (Miranda *et al.*, 2020).

The coefficient of permeability is of 6x10^{-4} m/s, which is within the usual range for clean sands. It was determined in a constant head permeameter, for a D_r of 70%, with the specimen completely saturated. The critical friction angle of the sand is of 36º, determined in triaxial tests. The sand has a Young's modulus, E, of 132 MPa and a Poisson's ratio, ν, of 0.3, determined in the initial phase of triaxial tests, with an axial strain up to 0.25% (Miranda, 2019).

2.2 *Expansive polyurethane resin MC-Injekt 2700 L®*

MC-Injekt 2700 L® is a low viscosity (approximately 200±50 mPa s), brown polyurethane-based resin, with a relatively long reaction time of about 45 min. It is a duromeric (closed cell) resin, with a high compressive strength of at least 75 MPa, and a high flexural tensile strength of around 65 MPa.

MC-Injekt 2700 L® consists of two components, which are mixed in the head of an injection pump with a ratio of 1:1, and, then, injected with adequate pressure and delivery rate. The mass density of the resin is approximately 1130 kg/m^3. Depending on the confining pressure, when in contact with water the resin can increase its volume up to 10 times, with a corresponding reduction in mass density.

2.3 *Specimen preparation*

A sand box was specifically designed in Perspex to prepare the sand before injection, i.e. to obtain the required D_r and to saturate it, reproducing closely the conditions at the Tagus River bed. The sand box dimensions were chosen to fit the existing sand shower, as well as to create a homogeneous volume of SRM which allows injection testing to be performed, without being affected by the boundary conditions (Figure 3a)). A small space was built below a bored plate at the bottom, to allow a uniform saturation of the sand mass. The net volume of the box is approximately 0.5x0.5x0.5 m^3. It was also designed to be easily open, with bolted connections between walls, bottom and top. The top four and the two lateral holes, below the bored plate, are closed by valves, to be used during saturation procedures.

The sand shower (Figure 3b)) was used to fill the sand box, with a certain D_r, in a systematic way and with assured repeatability. It is thoroughly described in Portugal (1999), but it is basically constituted by: a 0.375 m^3 parallelepipedal sand deposit; a drawer-type valve for regulating the sand flux; a motorized tilting hopper, which covers the area of the sand box to fill; a base to sustain the sand box; and four external transparent doors, to limit the propagation of sand dust.

The base of the deposit has a row of 0.01 m diameter holes in its central zone, which match with similar diameter holes of the drawer-type valve in the open position. Thus, by moving the drawer-type valve, the sand exit flow is controlled. The hopper's motion is controlled by a hydro-pneumatic system, which imposes a constant rate of displacement. Inside the hopper, there are three squared mesh nets, which disperse the sand, granting a uniform deposition, and stabilize grain descending trajectories, minimizing their mutual perturbation.

Therefore, after using the sand shower, the sand box was weighted, to determine the sand D_r. Subsequently, the top plate was tightened to the box and the saturation process was initiated. Firstly, the air in the specimen was removed and replaced by CO_2. CO_2 flowed through the specimen, from bottom to top, with each of the top valves open alternately during one hour. Then, de-aired water was injected in the two bottom valves and flowed to the top of the sand box, until CO_2 bubbles stopped exiting at each of the four top valves, ensuring the sand's full saturation (Figure 3c)).

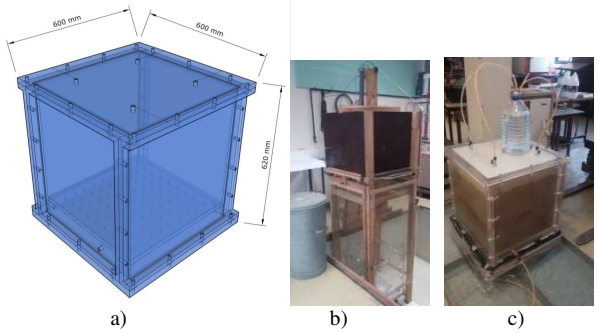

a) b) c)

Figure 3. a) Sand box; b) sand shower with box in place; c) water filling by upward flow.

The top plate was, then, removed and a rigid slab with 0.5x0.5 m^2 was placed over the sand. Several weights were uniformly distributed on this plate, constituting an average contact stress of 10 kPa (Figure 4). Applying this vertical stress was considered enough to confine the sand and, consequently, to enhance the SRM mechanical properties, in agreement with the findings of Traylen (2017), as well as reproduce in-situ injection conditions.

Next, the settlement of the sand was measured, based on the variation of the slab's top face vertical position, at the corners of the slab, as well as at the midpoints of the edges connecting them (8 control points).

After that, the injection rod was inserted into the sand and the resin injection was made while pulling out the rod, at the minimum operational pressure of the injector, around 100 kPa, to form SRM columns (Figure 4).

Figure 4. Load configuration (left); injection rod in the central position of the box (right).

Three injection tests were done. In the first test, a central column was injected. The second and third tests involved injecting five columns (Figure 5). The conical shape of the columns can be explained by the gravity effect and the viscosity of the resin.

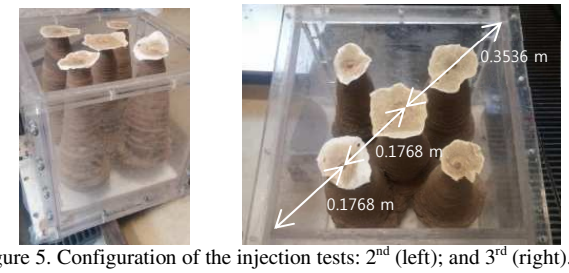

Figure 5. Configuration of the injection tests: 2nd (left); and 3rd (right).

The main goal of the first injection test was to characterize the physical and mechanical properties of the SRM. An injection rod withdrawal rate (IRWR) of 0.01 m/90 s was used. The second and third injection tests had the additional aim of measuring the effect of the injection on the sand densification between columns. The IRWR was of 0.01 m/10 s and 0.01 m/15 s for the second and third tests, respectively. The IRWR values were chosen after previous testing, to obtain a column diameter in accordance with the goals of each test, thus lower for the first test, to have more material to be core drilled, and higher for the second and third tests, to avoid overlapping of the columns.

After at least 3 hours, the settlement of the top slab was measured again. The sand around the SRM was excavated, dried and weighed. The volume and weight of the SRM were also measured. After 7 days the SRM columns were cut and core drilled to obtain the SRM specimens for laboratory testing. Before testing, the specimens were left curing inside water for at least another 7 days, to reproduce the conditions at the riverbed.

2.4 *Testing plan*

The physical and mechanical characterization of the SRM can be found in Miranda (2019). In short, the SRM behaves like a single-phase material. It has an average dry mass density of around 1800 kg/m^3. Its permeability is five orders of magnitude lower than the sand permeability. It exhibited an average uniaxial compressive strength of 31.0 MPa in the vertical direction and of 23.2 MPa in the horizontal direction, and a mean Young's modulus of around 5.0 GPa. For the critical state, a friction angle of 60.8° was obtained, being the critical shear strength independent of the IRWR. In the third injection test,

the sand's relative density had an absolute increase of 12.1% due to the resin injection.

Regarding the laboratory tests herein presented (four cyclic torsional tests), two specimens were core drilled, from the base and top of one SRM column of the second and third injection tests, respectively (Table 2). The diameters of the specimens were chosen taking into account the core drilling equipment available and to minimize the loss of SRM material.

Table 2. Tested specimens from the second and third injection tests

Specimen	Height (m)	External Radius (m)	Internal Radius (m)	p_{conf}* (kPa)
INJ2nd-B	0.1452	0.0372	0.0156	0
INJ2nd-T	0.1448	0.0372	0.0155	
INJ3rd-B	0.1431	0.0361	0.0156	
INJ3rd-T	0.1450	0.0372	0.0155	

*p_{conf} = confining stress.

2.5 *Equipment and testing conditions*

The GDS torsional shear device from the National Laboratory for Civil Engineering (LNEC) was used to perform cyclic torsional tests on hollow cylindrical specimens. This equipment is constituted by five fundamental units: a) the triaxial cell; b) the control/data acquisition system; c) the axial control system; d) the torsional control system; and e) the pressure and volume control system. The data acquisition system is formed by a personal computer, an interface, a signal conditioning system and five controllers, specifically: a digital controller of axial force/displacement; a digital controller of torque/rotation; and three controllers of water pressure/volumetric variation (internal pressure, external pressure and back pressure).The equipment is described in more detail in Serra (1998). In order to assure, as much as possible, uniformity of stress and strain states along the specimen, so that the corresponding measured average states would correspond to the real behaviour of the specimen, the porous plates at the top and bottom of the specimen were made with a high relief, enhancing friction and transmission of torsional rotation.

The specimens were placed at the torsional cell and were simply subjected to shear by controlling strain. Strain amplitude, $\gamma_{\theta z}$, was increased progressively, using each of the following values during 10 cycles, or until there was slipping at the top of the specimen: $\gamma_{\theta z} = \pm 5 \times 10^{-4}, \pm 1.0 \times 10^{-3}, \pm 3.0 \times 10^{-3}, \pm 4.5 \times 10^{-3}$. These values were chosen in accordance with the work previously done for the Tagus River sand (Miranda *et al.*, 2020). Similarly, to use a relevant frequency concerning earthquake loading, $f = 1$ Hz was chosen for the cyclic torsional tests herein presented.

3 ANALYSIS OF THE RESULTS

3.1 *Shear stress - shear strain behaviour of test INJ2nd-B*

The specimens were analysed in the elastic phase of their behavior. Figure 6 and Figure 7 illustrate the obtained results for test INJ2nd-B.

In Figure 6, it can be observed that up to cycle 30, with reduced cyclic strain amplitude, the cyclic curves are very close together, but, as the strains increase to the last imposed shear strain level, hysteresis loops' open up slightly. In fact, hysteresis loops' have a very steep slope, with a hysteresis area close to zero, as the specimens have a nearly elastic behaviour.

Actually, at cycle 31 there is a clear transition in the imposed amplitude of shear strain, which is then kept constant and equal to ±4.5x10^{-3} during 10 cycles, until the end of the test. This transition is also reflected in shear stress variation (Figure 7).

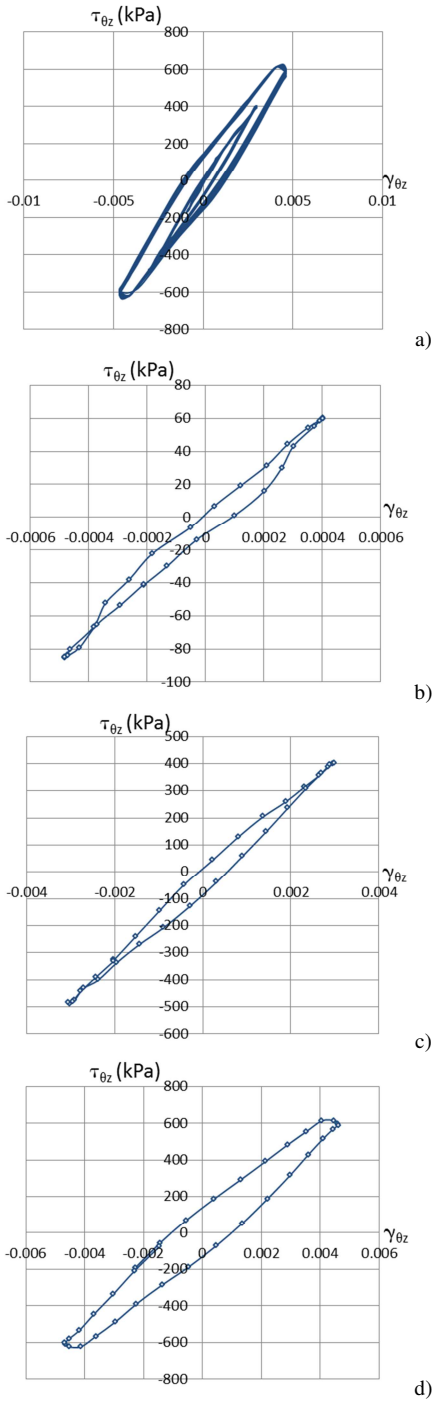

Figure 6. INJ2nd-B – Shear stress $\tau_{\theta z}$ (kPa) *versus* shear strain $\gamma_{\theta z}$: a) all cycles; b) cycle 6; c) cycle 26; d) cycle 36.

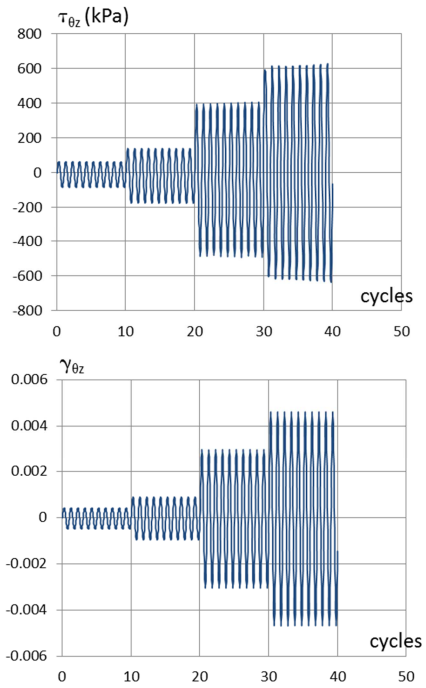

Figure 7. INJ2nd-B – Shear stress $\tau_{\theta z}$ (kPa) and shear strain $\gamma_{\theta z}$ *versus* number of cycles.

3.2 *Joint analysis of all tests*

3.2.1 *Equivalent shear modulus*

The equivalent shear modulus G_c is calculated for the first cycle, for each imposed shear strain level. The results are similar for the other cycles. At the beginning, there is an increase of G_c, which might be explained by the smaller precision in the shear strain measurements. Between an imposed shear strain of 1.0x10^{-3} and 3.0x10^{-3} the value of G_c is approximately constant. Finally, a slight reduction can be observed at the last level of imposed shear strain (4.5x10^{-3}) (Figure 8). At the initial shear strain of 5.0x10^{-4}, the values of G_c for the SRM are about 2 to 6 times the values of G_c for the sand alone. At the final shear strain of 4.5x10^{-3}, the difference increases to 9 to 16 times (Miranda *et al.*, 2020).

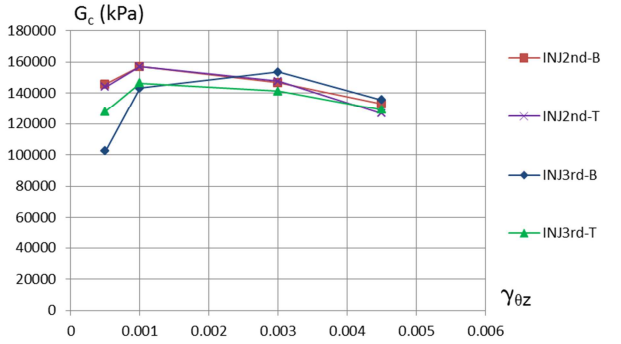

Figure 8. Equivalent shear modulus G_c (kPa) for the first cycle of each imposed shear strain level $\gamma_{\theta z}$.

3.2.2 *Damping ratio*

The damping ratio, ξ, is shown in Table 3, for the first cycle of each shear strain level. The results are similar for the other cycles. The values for the imposed shear strain levels of 5.0x10^{-4} and 1.0x10^{-3} are not presented here as they were affected by the calculation of the hysteresis area and are not realistic. In fact, a small error in the hysteresis area calculation may lead to a higher than expected value of ξ, as imposed strains are quite small. It is possible to observe that the damping ratio increases considerably from the imposed shear strain level of 3.0x10^{-3} to the imposed shear strain level of 4.5x10^{-3}, as expected. Comparing the SRM with the sand alone, in the latter case the value of ξ had already attained its peak and was already beginning to decrease, for the imposed shear strain level of 4.5x10^{-3} (Miranda *et al.*, 2020).

Table 3. Damping ratio ξ (%) (first cycle) *versus* $\gamma_{\theta z}$.

$\gamma_{\theta z}$	$\xi_{,INJ2nd-B}$ (%)	$\xi_{,INJ2nd-T}$ (%)	$\xi_{,INJ3rd-B}$ (%)	$\xi_{,INJ3rd-T}$ (%)
0.003	3.2	3.5	-	2.1
0.0045	15.0	14.7	16.1	11.6

4 CONCLUSIONS

An immersed tunnel case-study, supported on liquefiable alluvial Tagus river sands, was presented, providing context to this work. A novel liquefaction mitigation measure, namely injection of a duromeric (closed cell) expansive polyurethane resin, MC-Injekt 2700 L®, was tested. Three laboratory injection tests were executed: the first consisted in injecting a central column, inside a specifically designed box filled with Tagus River sand, to characterize the properties of the SRM; the second and third comprised injecting five separate columns each, with different replacement ratios, to measure the effect of the injection on the sand densification between columns. Four cyclic torsional tests were performed, using specimens from the base and top of the columns of the second and third injection tests. Imposed shear strain was increased progressively until there was slipping at the top of the specimen, considering strain amplitude levels with a limited number of cycles (10). The main goal of the tests was characterizing the cyclic behaviour of the SRM. The main findings of this study include:

- Between an imposed shear strain of 1.0x10^{-3} and 3.0x10^{-3} the value of G_c for the SRM is approximately constant. A slight reduction can be observed at the last level of imposed shear strain (4.5x10^{-3}). The values of G_c for the SRM are considerably higher than the values of G_c for the sand alone, particularly as the shear strain increases.
- In the case of the SRM, the damping ratio increases considerably from the imposed shear strain level of 3.0x10^{-3} to the imposed shear strain level of 4.5x10^{-3}, in contrast with the sand alone, where the value of ξ had already attained its peak and was already beginning to decrease, for the imposed shear strain level of 4.5x10^{-3}.
- The potential of this injection method, as a liquefaction mitigation method, has been demonstrated in what concerns improving the stiffness and the elastic behaviour of the Tagus River sand.

In the future, a technical and economical comparison of this liquefaction mitigation measure with other potential mitigation measures in immersed tunnels, such as the ones referred in chapter 1, will be performed. Based on this cost-benefit analysis, a consistent method to evaluate the performance of these measures may be developed, which will allow selecting the most adequate mitigation measure in design practice, for a specific site.

5 ACKNOWLEDGEMENTS

Luís Miranda was supported by "Fundação para a Ciência e Tecnologia" (FCT), through PhD scholarship SFRH/BD/99581/2014. MC-Bauchemie Portugal, in particular Nuno Silva, was paramount in the execution of the resin injections.

6 REFERENCES

ASTM. 2016. D4253-16: Standard Test Methods for Maximum Index Density and Unit Weight of Soils Using a Vibratory Table. *ASTM International*, West Conshohocken, PA, USA.

ASTM. 2016. D4254-16: Standard Test Methods for Minimum Index Density and Unit Weight of Soils and Calculation of Relative Density. *ASTM International*, West Conshohocken, PA, USA.

ASTM. 2017. D2487-17: Standard Practice for Classification of Soils for Engineering Purposes (Unified Soil Classification System). *ASTM International*, West Conshohocken, PA, USA.

Erdemgil, M., Saglam, S., and Bakir, B. 2007. Utilization of highly expansive polymer injection to mitigate seismic foundation failure for existing structures. *Proc. 8th Pacific Conference on Earthquake Engineering*, Nanyang Technological University, Singapore.

Ingerslev, C., and Kyiomya, O. 1997. Earthquake Analysis. *Tunnelling and Underground Space Technology* 12(2), 157–162.

Lunniss, R., and Baber, J. 2013. *Immersed tunnels*. CRC Press, Taylor & Francis Group, Boca Raton, Florida.

Manassero, M., Boffa, G., Dominijanni, A., and Puma, S. 2016. Injection of expanding polyurethane resins. *Proc. 24ª Conferenze di Geotecnica di Torino.* M. Manassero, A. Dominijanni, S. Foti, G. Musso, eds., Politecnico di Torino, 1–41.

Miranda, L. 2019. *Liquefaction Mitigation Measures: Prospective Application to Immersed Tunnel Foundations*. Ph.D. thesis, Universidade Técnica de Lisboa, Instituto Superior Técnico, Portugal.

Miranda, L., Caldeira, L., Serra, J. e Gomes, R. 2020. Dynamic behaviour of Tagus River sand including liquefaction. *Bulletin of Earthquake Engineering* 18(10), 4581-4604. Springer Nature. https://doi.org/10.1007/s10518-020-00881-5

Portugal, J. C. 1999. *Physical modelling with centrifuge* (in Portuguese). Ph.D. thesis, Universidade Técnica de Lisboa, Instituto Superior Técnico, Portugal.

Serra, J. B. 1998. *Experimental characterization and numerical modelling of the cyclic behaviour of non-cohesive soils. Application to earthquake engineering* (in Portuguese). Ph.D. thesis. Universidade Técnica de Lisboa, Instituto Superior Técnico, Portugal.

Skempton, A. W. 1986. Standard penetration test procedures and the effects in sands of overburden pressure, relative density, particle size, ageing and overconsolidation. *Géotechnique* 36, 425–447.

Traylen, N. 2017. *Resin injection ground improvement research trials*. Geotech Consulting ltd. Christchurch, New Zealand.

Uretek Worldwide. 2014. FAQ - about URETEK solutions. <http://www.uretekworldwide.com/> (Jan., 2019).